Journal of Microwaves, Optoelectronics and Electromagnetic Applications, Vol. 21, No. 3, September 2022
DOI: http://dx.doi.org/10.1590/2179-10742022v21i3262417

MGF Methods for Fixed and Gain Saturated Optically Preamplified FSO Links Impaired by Misalignments and Atmospheric Turbulence

Jeremiah Oluwatosin Bandele
Department of Design and New Media, School of Media and Communication (SMC), Pan-Atlantic University, Ibeju-Lekki, Lagos, P.O.Box 73688, Nigeria
jbandele@pau.edu.ng

***Abstract*— The Gaussian approximation is commonly used to evaluate the performance of free space optical communication systems. However, other performance evaluation methods such as the saddle point approximation, Chernoff bound and the modified Chernoff bound have also been used. This paper investigates the performance of fixed and gain saturated optically preamplified communication systems limited by factors such as strong atmospheric turbulence and pointing errors using various evaluation methods. Average bit error rate results are obtained over a range of average transmitted powers for free space optical communication systems without pointing error and those with pointing error using different saturation regimes, normalised beam widths and pointing error standard deviations. Results obtained in this paper show over a propagation distance of 1500 m, a receiver diameter of 0.15 m performed better than a receiver diameter of 0.03 m when the pointing error standard deviation is 0.1. Also, a receiver diameter of 0.03 m performed better than a receiver diameter of 0.15 m when the pointing error standard deviation is 4. These results show that while larger receiving lenses performed better when pointing error effects are minimal or absent, smaller receiving lenses are better when pointing error effects are dominant. Additionally, it is shown in this paper that while fixed and gain saturated optical preamplifiers produced similar performances when the decision threshold at the receiver is adaptive, the saddle point approximation is not useful for gain saturated optically preamplified receivers. Also, results in this paper showed optimal and near-optimal adaptive decision thresholds for the modified Chernoff bound and Gaussian approximation, respectively.**

***Index Terms*—** Atmospheric turbulence, free-space optical communication, modified Chernoff bound, optical amplifier, pointing error, saddle point approximation

I. Introduction

Free-space optical (FSO) communication systems have recently been established as viable alternatives to millimeter wave and radio frequency systems due to the various advantages they offer such as their use in difficult terrains (such as areas without right of way, across rail tracks or a river), ad hoc and multi-campus communication networks [1]–[3]. However, the impacts of atmospheric

Brazilian Microwave and Optoelectronics Society-SBMO *received 24 Mar 2022; for review 7 Apr 2022; accepted 28 July 2022*
Brazilian Society of Electromagnetism-SBMag *ISSN 2179-1074*

turbulence (AT) induced scintillation and pointing errors (PE) on system performance are key factors to consider when designing FSO communication systems. PEs occur in FSO communication systems due to issues such as imprecise tracking systems and vibrations produced by natural occurrences. Note that the ideal performance of FSO communication systems is negatively affected by AT and PEs [4], [5]. An optical amplifier (OA) is commonly used to mitigate losses due to scintillation and PE. Additionally, preamplifiers (OAs placed just before the receiver) are used to boost the photo-detector received power and improve the sensitivity of the receiver [6]. A key metric used to estimate the performance of FSO communication systems is the bit error rate (BER) [7]. While the Gaussian Approximation (GA) is a common and simple way of estimating the BER performance of optically preamplified receivers, several other methods have been developed to estimate the statistics (including the BER) of optically preamplified receivers. Such methods include the derivation of a moment generating function (MGF) for the photo-electron number, derivation of a characteristic function to give an approximate estimate of the BER, derivation of an analytical equation for the worst-case noise variance at the receiver output and the derivation of a MGF from the statistics of the detected signal [8]–[11]. An MGF approach of characterizing the signal and amplified spontaneous emission (ASE) noise is also used by the saddle point approximation (SPA), Chernoff bound (CB) and modified CB (MCB) to determine the BER [7].

By considering the OA's spontaneous emission noise, intersymbol interference, detection quantum noise, equalisation filter response and additive thermal noise, a novel MGF for an optically amplified receiver output signal was constructed in [7] for a non FSO communication scenario. The novel MGF in [7] was consistent with other previously established formulas and allowed for BER calculations using various limits and approximations. Results obtained from [7] showed that with low OA gain values, similar results are obtained for the SPA, GA and MCB while the CB gave an upper bound. At higher OA gain values, the MCB and the CB showed similar performances while the GA has a lower bound. It was concluded in [7] that the MCB is the preferred method for estimating the performance of the receiver. Some of the proposed methods in [7] was adapted for a FSO communication scenario in [12] where CB and MCB MGF-based approaches were used to obtain BER results for a on-off keying (OOK) optically preamplified FSO communication system operating in a turbulent atmosphere. The findings in [12] with the MGF methods were compared to the GA technique for both low and high preamplifier gains in the weak to saturated AT regimes and in comparison with the CB, the MCB was shown to provide the tightest bound on the BER, especially when using preamplifiers with lower gain values. In the FSO communication system with digital pulse position modulation (DPPM) and optical preamplification considered in [13] where the effects of AT and PE on system performance was analysed, it was shown that the combined impairments have a negative impact on the overall performance of the FSO system. Also, for the various scenarios considered in [13], FSO communication systems utilising the DPPM modulation scheme were considerably more power efficient than the FSO communication systems utilising non-return-to-zero (NRZ) OOK modulation.

Brazilian Microwave and Optoelectronics Society-SBMO received 24 Mar 2022; for review 7 Apr 2022; accepted 28 July 2022
Brazilian Society of Electromagnetism-SBMag ISSN 2179-1074

In [14], novel lower and upper bounds were developed for the average error probability of optical communication systems impaired by factors such as avalanche gain and intersymbol interference using direct detection. While the bound in [14] performed better than the CB, it is more complicated to develop and therefore only preferable in applications where additional complexity can be accommodated to provide for more accuracy. The use of M-ary DPPM M-pulse amplitude and position modulation (M-PAPM) to deliver more bits and improve efficiency was shown in [15] for a hybrid fiber/FSO (HFFSO) communication system consisting of a dense WDM (DWDM) passive optical network (PON) and an OOK/M-ary DPPM-M-PAPM. The introduction of digital signal processed adaptive optics (AO) in [15] resulted in reduced interchannel crosstalk and improved reliability. Also, the OOK/M-ary DPPM-M-PAPM improved the spectral efficiency. The analysis in [15] included the use of evaluation methods such as the GA, CB and MCB. The results obtained in [15] show that compared to the OOK-NRZ scheme, the proposed M-ary DPPM-M-PAPM scheme is more reliable and offers improved receiver sensitivity. The CB and MCB used an MGF approach for BER evaluations in [16] where the impact of aperture averaging, interchannel crosstalk, geometric spread, PE and ASE noise on DPPM, OOK, M-ary spatial modulation (SM)/PPM and M-ary PPM FSO communication systems was analysed. The AT channel was modelled with the K-distribution and the gamma-gamma (GG) distribution. The results obtained in [16] showed that the proposed model offers benefits such as power efficiency and enhanced system performance (with reduced bandwidth efficiency). Also as expected, the use of many receivers and/or transmitters was shown in [16] to improve system performance.

Since the effects of AT on the performance of FSO communication systems are strongly significant in the strong to saturated AT regimes [17], it is advantageous to develop models and evaluate system performance in the strong to saturated AT regimes since the results obtained would serve as upper bounds to those obtainable in AT regimes with lower strengths. In this paper, the performance of fixed (OAs that are not allowed to go into gain saturation) and gain saturated (OAs that are allowed to go into gain saturation) optically preamplified FSO communication systems limited by ASE noise, strong AT, geometric spread (GS) and PEs are evaluated by using the SPA, GA and MCB (since the MCB is known to provide a tighter bound compared to the CB [7], [12]) methods with an adaptive decision threshold. Note that the MCB and SPA evaluation methods use an MGF approach to obtain the BER. Also by considering the effects of strong AT, ASE noise and PEs over various decision threshold levels using the GA, MCB, and the SPA methods, the optimal adaptive decision threshold is shown. Note that while related works have focused on evaluating system performance with the GA, the use of MGF methods to approximate the bit error rate has been shown to give more accurate estimates compared to the GA because they give better representations of the signal and noise components. While the actual BER is not known, MGF methods such as the MCB provide an upper bound on the BER and can be regarded as being more accurate than the GA because there is uncertainty about when the GA values are higher or lower than the actual BER [7], [12]. After this

DOI: http://dx.doi.org/10.1590/2179-10742022v21i3262417

introductory part, the atmospheric channel is described in section II followed by a FSO communication system model description in section III. Section IV contains the BER analysis using the SPA, GA and MCB performance evaluation methods. The results and discussion part of this work is provided in section V, followed by a conclusion in section VI.

II. The Atmospheric Channel

Different statistical distributions have been developed to describe various regimes of AT. A particular AT model known to adequately describe various AT regimes (including the strong AT regime) is the GG distribution, with an unconditional PDF defined as [1], [17]

$$f_{GG}(h_t) = \frac{2(\alpha\beta)^{(\alpha+\beta)/2}}{\Gamma(\alpha)\Gamma(\beta)} h_t^{\left(\frac{\alpha+\beta}{2}\right)-1} K_{\alpha-\beta}\left(2\sqrt{\alpha\beta h_t}\right) \quad h_t > 0 \tag{1}$$

where h_t is the fluctuating channel gain (or loss) due to the turbulent atmosphere. $K_u(.)$ and $\Gamma(.)$ are the second kind modified Bessel function having order u and the gamma function respectively. With a plane wave assumption for the incident wave, α and β are defined as [17]

$$\alpha = 1\Big/\left\{\exp\left[\frac{0.49\sigma_R^2}{\left(1+\left(1.11\sigma_R^{12/5}\right)\right)^{7/6}}\right]-1\right\} \tag{2}$$

$$\beta = 1\Big/\left\{\exp\left[\frac{0.51\sigma_R^2}{\left(1+\left(0.69\sigma_R^{12/5}\right)\right)^{5/6}}\right]-1\right\} \tag{3}$$

where $\sigma_R^2 = 1.23D^{11/6}k^{7/6}C_n^2$ is the Rytov variance. C_n^2 and D are the refractive index structure parameter and FSO communication system propagation distance respectively. The optical wave number with wavelength λ is defined as $k=2\pi/\lambda$. By including the effects of diffraction and AT, the width of the Gaussian beam at a distance z, is defined as [1]

$$w_z \approx w_{z_d}\sqrt{1+1.33\sigma_R^2\left(2z/kw_{z_d}\right)^{5/6}} \tag{4}$$

where $w_{z_d} = w_0\sqrt{1+\left(z/z_R\right)^2}$ is the width of the beam while only considering diffraction effects, w_0 is the waist of the beam at $z=0$ and $z_R = \pi w_0^2/\lambda$ is the Raleigh range. A Raleigh distribution model can be used to adequately describe the combination of GS, PE and AT. Also by using a Raleigh distribution model to adequately describe the combination of the GS and PE and with the assumption of a circular receiver aperture, the fluctuating channel gain (or loss) due to GS and PE has a PDF given as [18], [19]

$$f_{h_p}\left(h_p\right) = h_p^{\varsigma^2-1}\frac{\varsigma^2}{a_0^{\varsigma^2}}, \qquad a_0 \ge h_p \ge 0 \tag{5}$$

where $\varsigma = w_{z_{eq}}/2\sigma_{PE}$. σ_{PE} is the standard deviation of the PE displacement at the optical receiver, $a_0=\left[erf(\upsilon)\right]^2$ is the fraction of the collected power at the receiving lens at $r=0$ where r is the

  ISSN 2179-1074

receiver radius and h_p is the fluctuating channel gain (or loss) due to GS and PE. $w_{z_{eq}} = w_z\sqrt{\sqrt{\pi}erf(\upsilon)/2\upsilon\exp(-\upsilon^2)}$ is the equivalent beam where $\upsilon = \sqrt{\pi}r_{rx}/\sqrt{2}w_z$. Now, by including the effects of GS and PE, the GG distribution PDF is defined as [13]

$$f_h(h) = \frac{2\varsigma^2(\alpha\beta)^{(\alpha+\beta)/2}}{a_0^{\varsigma^2}\Gamma(\alpha)\Gamma(\beta)} h^{\varsigma^2-1} \int_{h/a_0}^{\infty} h_t^{\left(\frac{\alpha+\beta}{2}\right)-1-\varsigma^2} K_{\alpha-\beta}\left(2\sqrt{\alpha\beta h_t}\right)dh_t \quad (6)$$

Note that $h = h_t h_p$ is the fluctuating channel gain (or loss) due to the turbulent atmosphere, GS and PE.

III. FSO Communication System Model

A FSO communication system using NRZ-OOK with direct detection and a preamplified optical receiver is shown in Fig. 1. It is assumed that the receiver is not perfectly aligned with the transmitter. After the scintillated optical signal reaches the receiver, it is passed through an optical preamplifier. Since optical amplification generates ASE noise, an optical band pass filter (OBPF) is placed after the OA for ASE noise reduction before a photodiode (PD) converts the optical signal into an electrical signal. The PD has a responsivity $R = q\eta/vh$ where v , η , h and q are the optical carrier frequency, quantum efficiency, Planck constant and electronic charge respectively. Then, with the help of a synchronisation system, a decision circuit is used to retrieve the information sent from the transmitting end [6], [17].

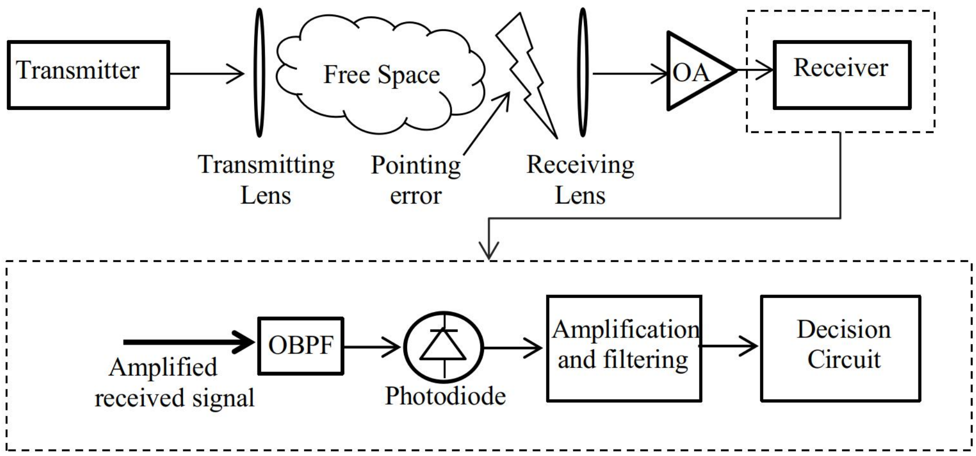

Fig. 1. FSO communication system model with PE and a preamplified optical receiver

IV. BER Analysis

The BER analysis of the FSO communication system is evaluated by using the GA and MGF approaches such as the SPA and the MCB [7], [12]

A. Gaussian Approximation

With an assumption that the noise is Gaussian, the BER is defined as [6]

ISSN 2179-1074

$$BER\left(P_{OAin_{av}},h\right)=\frac{1}{2}\left[\frac{1}{2}\text{erfc}\left(\frac{i_{D_{GA}}\left(P_{OAin_{av}},h\right)-i_0\left(P_{OAin_{av}},h\right)}{\sqrt{2\sigma_0^2\left(P_{OAin_{av}},h\right)}}\right)+\frac{1}{2}\text{erfc}\left(\frac{i_1\left(P_{OAin_{av}},h\right)-i_{D_{GA}}\left(P_{OAin_{av}},h\right)}{\sqrt{2\sigma_1^2\left(P_{OAin_{av}},h\right)}}\right)\right] \tag{7}$$

where $i_x = GRP_{OAin_x}$ is the average signal level when sampling takes place with $x \in \{0,1\}$ being the data bits that were transmitted. $P_{OAin_1} = \frac{2e_r}{e_r+1}P_{OAin_{av}}$ and $P_{OAin_1} = \frac{2}{e_r+1}P_{OAin_{av}}$ are powers in 1 and 0 bits respectively. $P_{OAin_{av}}$, $e_r = P_{OAin_1}/P_{OAin_0}$ and G are the OA input mean power, extinction ratio and OA gain respectively. $\sigma_x^2 = \sigma_{sx-sp}^2 + \sigma_{sp-sp}^2 + \sigma_{th}^2$ is the complete noise current variance where $\sigma_{sx-sp}^2 = 4GR^2P_{OAin_x}N_0B_e$ and $\sigma_{sp-sp}^2 = 2m_tR^2N_0^2B_{opt}B_e\left(1-\frac{B_e}{2B_{opt}}\right)$ are the signal-spontaneous and spontaneous-spontaneous beat noises respectively. σ_{th}^2, B_{opt}, m_t, $N_0 = \frac{1}{2}(NFG-1)hv$ and $B_e = 0.7R_b$ are the receiver thermal noise variance, OBPF bandwidth, polarisation states parameter number, ASE noise power spectral density and receiver noise equivalent bandwidth respectively. NF and R_b are the noise figure and bit rate respectively. For the adaptive decision threshold considered in this work, the decision threshold (assumed to vary with h) is given as [6]

$$i_{D_{GA}}\left(P_{OAin_{av}},h\right)=\frac{i_1\left(P_{OAin_{av}},h\right)\sigma_0\left(P_{OAin_{av}},h\right)+i_0\left(P_{OAin_{av}},h\right)\sigma_1\left(P_{OAin_{av}},h\right)}{\sigma_1\left(P_{OAin_{av}},h\right)+\sigma_0\left(P_{OAin_{av}},h\right)} \tag{8}$$

Note that when the OA experiences gain saturation, G changes proportionally to the OA input power as described in [6], [20].

B. MGF Methods

The MGF of an optical signal, which also accounts for the ASE noise, is given by [7], [12]

$$M_{Y_x}(P_{OAin_{av}},s) = \frac{e^{\frac{RG_{ss}sP_{OAin_x}(P_{OAin_{av}})}{1-(RN_0s/T)}}}{\left(1-(RN_0\,s/T)\right)^L} \tag{9}$$

where s is a standard parameter in the MGF transform domain, $L = B_{opt}m_tT$ and T is the bit period. By including the effect of thermal noise, the MGF is given by [7], [12]

$$M_{Z_x}(P_{OAin_{av}},s) = M_{th}(s)M_{Y_x}(P_{OAin_{av}},s) \tag{10}$$

where the thermal noise MGF, $M_{th}(s) = e^{\frac{\sigma_{th}^2s^2}{2}}$.

The MCB which gives a tighter bound on the BER (compared to the CB), is given as [7], [12]

$$BER_{MCB}(P_{OAin_{av}},s_0\,|\,h,s_1\,|\,h)=\frac{1}{2}\left[\frac{e^{-s_0i_{D_{MCB}}(P_{OAin_{av}},s_0|h)}M_{Z_0}(P_{OAin_{av}},s_0\,|\,h)}{s_0\sqrt{2\pi\sigma_{th}^2}}+\frac{e^{s_1i_{D_{MCB}}(P_{OAin_{av}},s_1|h)}M_{Z_1}(P_{OAin_{av}},-s_1\,|\,h)}{s_1\sqrt{2\pi\sigma_{th}^2}}\right] \tag{11}$$

The SPA, is given as [7]

  ISSN 2179-1074

$$BER_{SPA}(P_{OAin_{av}},s_0\,|\,h,s_1\,|\,h)=\frac{1}{2}\left[\frac{e^{-s_0 i_{D_{SPA}}(P_{OAin_{av}},s_0|h)}M_{Z_0}(P_{OAin_{av}},s_0\,|\,h)}{s_0\sqrt{2\pi\psi_0''(P_{OAin_{av}},-s_0\,|\,h)}}+\frac{e^{s_1 i_{D_{SPA}}(P_{OAin_{av}},s_1|h)}M_{Z_1}(P_{OAin_{av}},-s_1}{s_1\sqrt{2\pi\psi_1''(P_{OAin_{av}},s_1\,|\,h)}}\right. \quad (12)$$

where functions $\psi_0(P_{OAin_{av}},-s_0\,|\,h)$ and $\psi_1(P_{OAin_{av}},s_1\,|\,h)$ are given by

$$\psi_0(P_{OAin_{av}},-s_0\,|\,h)=\ln\left[\frac{e^{-s_0 i_{D_{SPA}}(P_{OAin_{av}},s_0|h)}M_{Z_0}(P_{OAin_{av}},s_0\,|\,h)}{s_0}\right] \quad (13)$$

$$\psi_1(P_{OAin_{av}},s_1\,|\,h)=\ln\left[\frac{e^{s_1 i_{D_{SPA}}(P_{OAin_{av}},s_1|h)}M_{Z_1}(P_{OAin_{av}},-s_1\,|\,h)}{s_1}\right] \quad (14)$$

A near optimal adaptive decision threshold for the MCB can be obtained by differentiating the CB BER (provided in [7]) with respect to the decision threshold and equating the result to zero [7], [12], [14]. By conditioning the result on h, the near optimal adaptive decision threshold for the MCB is given as [7], [14].

$$i_{D_{MCB}}(s_0\,|\,h,s_1\,|\,h,P_{OAin_{av}})=\ln\left(\frac{s_0 M_{Y_0}(P_{OAin_{av}},s_0\,|\,h)}{s_1 M_{Y_1}(P_{OAin_{av}},-s_1\,|\,h)}\right)\Big/(s_0+s_1) \quad (15)$$

Note that the adaptive decision threshold in (15) is also applicable to the SPA. Even though tighter bounds are obtained by optimising s_0 and s_1 separately, it is computationally convenient to set $s=s_0=s_1$. By setting $s_0=s_1=s>0$, (11) and (12) can be rewritten as

$$BER_{MCB}(P_{OAin_{av}},s\,|\,h)=\frac{1}{2}\left[\frac{e^{\frac{\sigma_{th}^2 s^2}{2}+\frac{RG_{ss}sP_{OAin_0}(P_{OAin_{av}},h)}{1-(RN_0 s/T)}-i_{D_{MCB}}(P_{OAin_{av}},s|h)}}{(1-(RN_0\,s/T))^L s\sqrt{2\pi\sigma_{th}^2}}+\frac{e^{\frac{\sigma_{th}^2 s^2}{2}-\frac{RG_{ss}sP_{OAin_1}(P_{OAin_{av}},h)}{1+(RN_0 s/T)}+i_{D_{MCB}}(P_{OAin_{av}},s|h)}}{(1+(RN_0\,s/T))^L s\sqrt{2\pi\sigma_{th}^2}}\right] \quad (16)$$

$$BER_{SPA}(P_{OAin_{av}},s\,|\,h)=\frac{1}{2}\left[\frac{e^{\frac{\sigma_{th}^2 s}{2}+\frac{RG_{ss}P_{OAin_0}(P_{OAin_{av}},h)}{1-(RN_0 s/T)}-i_{D_{SPA}}(P_{OAin_{av}},s|h)}}{(1-(RN_0\,s/T))^L\sqrt{2\pi\psi_0''(P_{OAin_{av}},-s\,|\,h)}}+\frac{e^{\frac{\sigma_{th}^2 s}{2}-\frac{RG_{ss}P_{OAin_1}(P_{OAin_{av}},h)}{1+(RN_0 s/T)}+i_{D_{SPA}}(P_{OAin_{av}},s|h)}}{(1+(RN_0\,s/T))^L\sqrt{2\pi\psi_1''(P_{OAin_{av}},s\,|\,h)}}\right. \quad (17)$$

where

$$\psi_0(P_{OAin_{av}},-s\,|\,h)=\frac{\sigma_{th}^2 s}{2}+\frac{RG_{ss}P_{OAin_0}(P_{OAin_{av}},h)}{1-(RN_0\,s/T)}-i_{D_{SPA}}(P_{OAin_{av}},s\,|\,h)-\ln\left[\frac{1}{(1-(RN_0\,s/T))^L}\right] \quad (18)$$

And

$$\psi_1(P_{OAin_{av}},s\,|\,h)=\frac{\sigma_{th}^2 s}{2}-\frac{RG_{ss}P_{OAin_1}(P_{OAin_{av}},h)}{1+(RN_0\,s/T)}+i_{D_{SPA}}(P_{OAin_{av}},s\,|\,h)-\ln\left[\frac{1}{(1+(RN_0\,s/T))^L}\right] \quad (19)$$

Also, the near optimal adaptive decision threshold for the MCB and SPA can be rewritten as

$$i_{D_{MCB/SPA}}(P_{OAin_{av}}, s \mid h) = \frac{\frac{RG_{ss}sP_{OAin_0}(P_{OAin_{av}}, h)}{1-(RN_0\, s/T)} + \frac{RG_{ss}sP_{OAin_1}(P_{OAin_{av}}, h)}{1+(RN_0\, s/T)} + \ln\left[\frac{(1+(RN_0\, s/T))^L}{(1-(RN_0\, s/T))^L}\right]}{2s} \tag{20}$$

C. Average BER

To obtain the average BER, the instanteneous BER can be statically averaged over h and given as [12]

$$BER_{EM_{av}}\left(P_{OAin_{av}}\right) = \int_0^\infty BER_{EM}\left(P_{OAin_{av}}, h\right) f_h(h) dh \tag{21}$$

where $EM \in \{GA, MCB, SPA\}$ is the performance evaluation method used to obtain the instantaneous BER. The optimal adaptive decision threshold can then be determined by assuming that (8) and (20) is equivalent to when a normalised decision threshold is situated midway between the 1 and 0 bits (i.e. D_{rel} = 0.5) and then varying D_{rel} to obtain the optimal adaptive decision threshold, expressed as

$$i_{D_{EM,opt}} = \Lambda\left(BER_{EM_{av},D_{rel}}\left(P_{OAin_{av}}\right)\right) \qquad D_{rel} \in \left\langle 0,...,0.5,...,1 \middle| P_{OAin_{av}} \right\rangle \tag{22}$$

Note that the optimal adaptive decision threshold will be the D_{rel} that gives the best BER performance for a particular $P_{OAin_{av}}$.

V. Results and Discussions

The parameters used for the numerical analysis are shown in Table I. Considering the propagation distance of 1500 m assumed in this work, the strong atmospheric turbulence regime is modelled with σ_R^2 = 3.5 ($C_n^2 = 8.36 \times 10^{-14} m^{-2/3}$). Also, with a beam divergence angle of 1.5×10^{-4} rad and beam waist (at $D = 0$), w_0 = 0.002, receiver diameters d = 0.15 m and d = 0.03 m will give normalised beam widths of W_z/r = 5 and W_z/r = 25 respectively. For the numerical analysis, OAs that are not allowed to achieve gain saturation and OAs that are allowed to achieve gain saturation are called fixed gain ($P_{sat} \to \infty$) and gain saturated (P_{sat} = 5 dBm) OAs respectively. Also, in addition to the inclusion of ASE noise effects, the OA is allowed to freely respond with complete saturation characteristic. GE and PE effects are considered for cases with normalised beam widths, $W_z/r \in \{5, 25\}$ and PE standard deviation, $\sigma_{PE} \in \{0.1, 4\}$. Note that the BER performances obtained are deemed acceptable if they fall within limits where forward error correction can be applied.

By using the SPA, GA and MCB evaluation methods and including GS, PE and AT effects, the average BER obtained in a FSO communication system over a range of average transmitted powers is shown in Fig. 2. The FSO communication systems analysed are those without PE (WoPE) and with PE (WPE) using different σ_{PE}, P_{sat} and W_ξ/r values. Note that while most commercial free space optics devices have transmitted powers higher than 0dBm, we have presented results for transmitted powers lower than 0dBm because the results presented provide upper bounds on the BER for higher

Brazilian Microwave and Optoelectronics Society-SBMO received 24 Mar 2022; for review 7 Apr 2022; accepted 28 July 2022
Brazilian Society of Electromagnetism-SBMag

ISSN 2179-1074

transmitted powers and also gives FSO system designers the opportunity to see what is achievable with lower transmitted powers.

TABLE I. NUMERICAL ANALYSIS PARAMETERS

Parameter	Symbol	Value
OA small signal gain	G_{ss}	30 dB [21]
Noise figure	NF	5 dB [12]
Bit rate	R_b	2.5 Gb/s [21]
Optical wavelength	λ	1550 nm [6], [21]
OBPF bandwidth	B_{opt}	76 GHz [22]
Receiver thermal noise	σ_{th}	7×10^{-7} A [12]
Extinction ratio	e_r	10 dB [12]
Quantum efficiency	η	0.8 [2]

Average BER results for the SPA, GA and MCB are shown for FSO communication systems WoPE ($P_{sat} \in \{5dBm, \infty\}$, $W_z/r = 5$) and WPE ($P_{sat} \in \{5dBm, \infty\}, \sigma_{PE} = 0.1$, $W_z/r = 5$) in Fig. 2a.

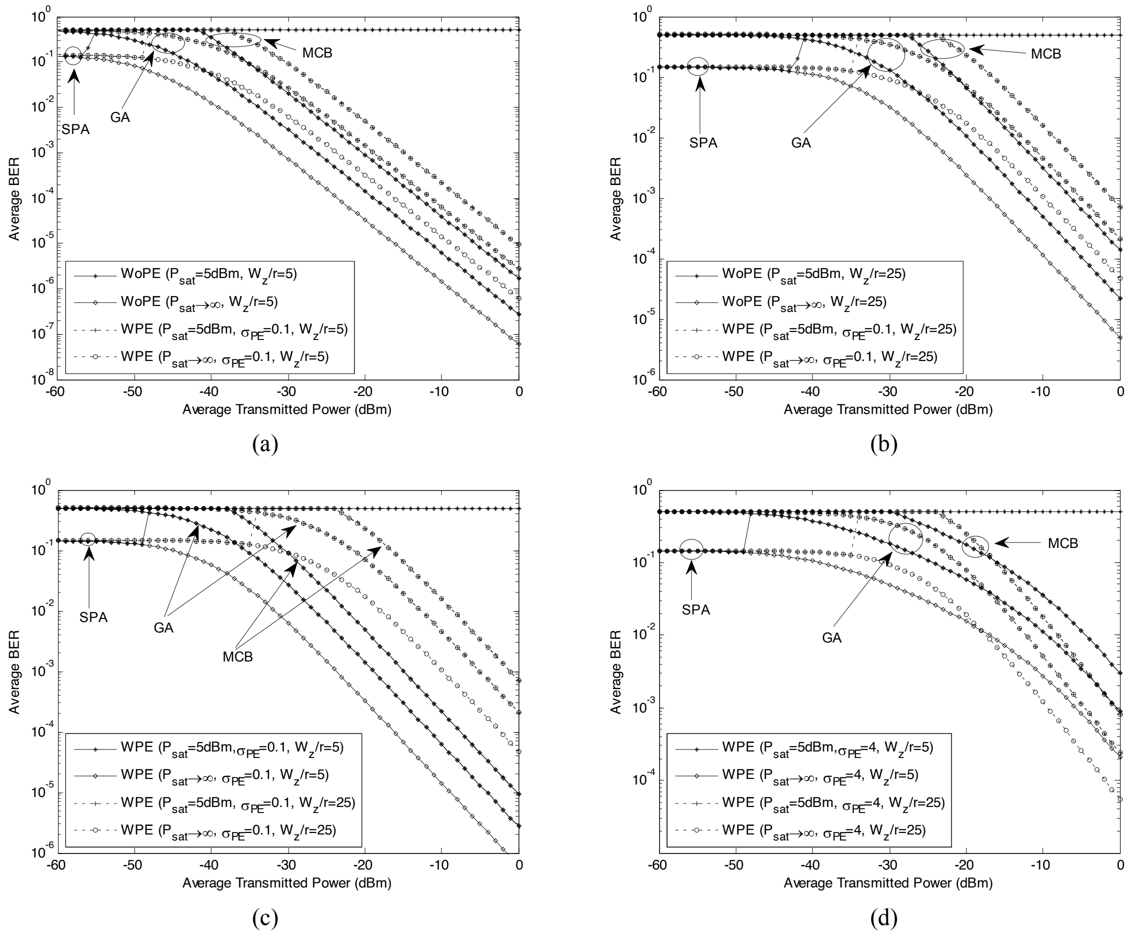

Fig. 2 Average BER over a range of average transmitted powers for SPA, GA and MCB performance evaluation methods; including GS, PE and AT effects. $P_{sat} \in \{5dBm, \infty\}$
(a) WoPE ($W_z/r = 5$) and WPE ($\sigma_{PE} = 0.1$, $W_z/r = 5$) (b) WoPE ($W_z/r = 25$) and WPE ($\sigma_{PE} = 0.1$, $W_z/r = 25$)) (c) WPE ($\sigma_{PE} = 0.1$, $W_z/r \in \{5, 25\}$) (d) WPE ($\sigma_{PE} = 4$, $W_z/r \in \{5, 25\}$)

When $P_{sat} \to \infty$, the SPA performed better than the GA and the MCB; with the MCB recording the least performance. Note that these results do not invalidate the use of the MCB in FSO

Brazilian Microwave and Optoelectronics Society-SBMO received 24 Mar 2022; for review 7 Apr 2022; accepted 28 July 2022
Brazilian Society of Electromagnetism-SBMag

ISSN 2179-1074

communication systems because the MCB, which has been known to give comparable and upper bounds on the GA with low and high gain preamplifiers respectively [12], [15], has been proposed as a preferred performance evaluation method [7], [12]. Also, systems WoPE (W_z/r = 5) performed better than systems WPE (σ_{PE} = 0.1, W_z/r = 5); which is expected since the presence of PE limits the performance of systems WPEs. Average BER results for the SPA, GA and MCB shown for FSO communication systems WoPE ($P_{sat} \in \{5dBm, \infty\}$, W_z/r = 25) and WPE ($P_{sat} \in \{5dBm, \infty\}$, σ_{PE} = 0.1, W_z/r = 25) in Fig. 2b when $P_{sat} \to \infty$ are also similar to those obtained in Fig. 2a in terms of the overall performance of each performance evaluation method. Also as expected, systems WoPE (W_z/r = 25) performed better than systems WPE (σ_{PE} = 0.1, W_z/r = 25) in Fig. 2b.

Average BER results for the SPA, GA and MCB are shown for FSO communication systems WPE ($P_{sat} \in \{5dBm, \infty\}$, σ_{PE} = 0.1, $W_z/r \in \{5, 25\}$) and WPE ($P_{sat} \in \{5dBm, \infty\}$, σ_{PE} = 4, $W_z/r \in \{5, 25\}$) in Fig. 2c and Fig. 2d respectively where the SPA also performed better than the GA and the MCB. However, while W_z/r = 5 consistently performed better than W_z/r = 25 when σ_{PE} = 0.1 as seen in Fig. 2c, W_z/r = 5 only performed better than W_z/r = 25 with lower transmitted powers ($<$ -18dBm, $<$ -17dBm, and $<$ -16dBm for the SPA, GA and MCB respectively) in Fig. 2d where σ_{PE} = 4. With higher transmitted powers values ($>$ -18dBm, $>$ -17dBm, and $>$ -16dBm for the SPA, GA and MCB respectively) in Fig. 2d where σ_{PE} = 4, W_z/r = 25 performed better than W_z/r = 5. These results (in conformity with **[13]**) show that while larger receiving lenses produce better performances compared to smaller receiving lenses when PE effects are minimal or absent, smaller receiving lenses are preferable when PE effects are significant. It is noteworthy that while OA gain saturation is known to reduce the G_{ss} **[6], [20]**, results in Figs. 2a, 2b and 2c showed similar performances when P_{sat} = 5 dBm (for the GA and MCB) and $P_{sat} \to \infty$. These results show that the reduction in the G_{ss} due to increased transmitted powers has no effect on system performance when the decision threshold at the receiver is adaptive; both for the GA and MCB evaluation methods. However, the SPA only gave useful results for $P_{sat} \to \infty$ and not for P_{sat} = 5 dBm, meaning that the SPA is not useful for gain saturated preamplifiers.

The minimum average BER (including GS, PE and AT effects) obtained in a FSO communication system with performance evaluation methods such as the SPA, GA and MCB over a range of normalised decision thresholds WoPE ($P_{sat} \in \{5dBm, \infty\}$, $W_z/r \in \{5, 25\}$) and WPE ($P_{sat} \in \{5dBm, \infty\}$, $\sigma_{PE} \in \{0.1, 4\}$, $W_z/r \in \{5, 25\}$) are shown in Fig. 3 for transmitted power P_t = 10dBm. In Fig. 3a, 3b and 3c where the SPA, GA and MCB performance evaluation methods are used respectively, results obtained for each evaluation method aligns with findings in Fig. 2 that while

Brazilian Microwave and Optoelectronics Society-SBMO received 24 Mar 2022; for review 7 Apr 2022; accepted 28 July 2022
Brazilian Society of Electromagnetism-SBMag *ISSN 2179-1074*

similar performances are obtained when $P_{sat} \to \infty$ and P_{sat} = 5 dBm for the GA and MCB, the SPA only gives useful results when $P_{sat} \to \infty$.

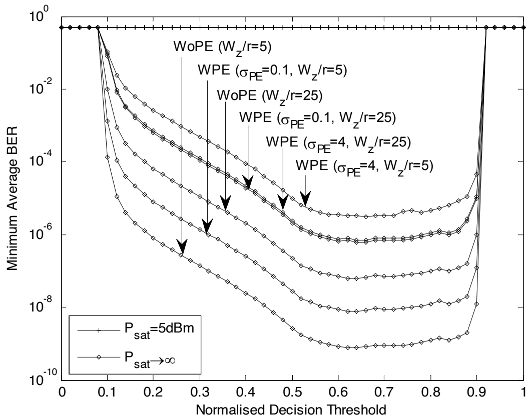

(a)

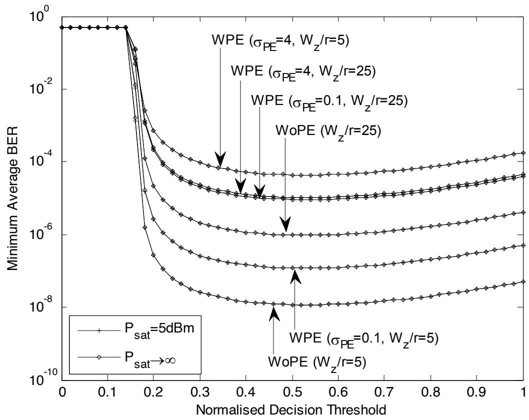

(b)

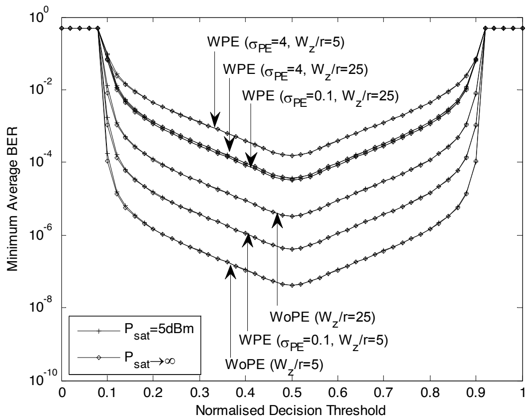

(c)

Fig. 3 Minimum average BER over a range of normalised decision thresholds WoPE ($W_z/r \in \{5, 25\}$) and WPE ($\sigma_{PE} \in \{0.1, 4\}$, $W_z/r \in \{5, 25\}$); including GS, PE and AT effects. $P_{sat} \in \{5dBm, \infty\}$
(a) SPA (b) GA (c) MCB

Also, with each evaluation method, the performance level of the FSO communication systems under consideration in descending order are systems WoPE ($P_{sat} \in \{5dBm, \infty\}$, W_z/r = 5), systems WPE ($P_{sat} \in \{5dBm, \infty\}$, σ_{PE} = 0.1, W_z/r = 5), systems WoPE ($P_{sat} \in \{5dBm, \infty\}$, W_z/r = 25), systems WPE ($P_{sat} \in \{5dBm, \infty\}, \sigma_{PE}$ = 0.1, W_z/r = 25), systems WPE ($P_{sat} \in \{5dBm, \infty\}, \sigma_{PE}$ = 0.4, W_z/r = 25) and systems WPE ($P_{sat} \in \{5dBm, \infty\}$, σ_{PE} = 0.4, W_z/r = 5). These results show (in alignment with Fig. 2) that while larger receiving lenses are preferable when PE effects are minimal or absent, smaller receiving lenses perform better when PE effects are significant. The MCB results in Fig. 3c show that the adaptive threshold in (20) which represents D_{rel} = 0.5 is optimal since minimum average BERs are consistently obtained at D_{rel} = 0.5. For the GA in Fig. 3b, the results align with [6] that the adaptive threshold in (15) which represents D_{rel} = 0.5 is only near-optimal since minimum average BERs are not clearly obtained at D_{rel} = 0.5. Minimum average BER results for the SPA in Fig.

  ISSN 2179-1074

3a also shows that the adaptive threshold in (20) which represents D_{rel} = 0.5 is not optimal for the SPA because the minimum average BERs obtained at D_{rel} = 0.5 are not optimal for all the FSO communication systems under consideration.

VI. Conclusion

This paper considered the performance of fixed and gain saturated optically preamplified FSO communication systems limited by ASE noise, strong AT, GS and PEs using evaluation methods such as the SPA, GA and MCB with an adaptive decision threshold. The optimal adaptive decision thresholds for the FSO communication systems under consideration are also presented. It was shown in this paper that, as expected, FSO communication systems WoPE performed better than FSO communication systems WPE and that, with high gain preamplifiers, MCBs are upper bounds on the GA. Also, this paper showed that when PE effects are minimal or absent, larger receiving lenses perform better than smaller receiving lenses. However, smaller receiving lens produced better performances when PE effects are dominant. In this paper, it was shown that even though gain saturation results in reduced OA gain, comparable performances were observed in systems with fixed and gain saturated optical preamplifiers when the decision threshold at the receiver is adaptive. Also based on the obtained results, the adaptive decision thresholds used in this paper proved to be optimal, near-optimal and not optimal for the MCB, GA and SPA respectively.

References

[1] L. C. Andrews and R. L. Phillips, *Laser Beam Propagation Through Random Media*. SPIE Optical Engineering Press, 1998.

[2] A. K. Majumdar, "Free-space laser communication performance in the atmospheric channel," *J Optic Comm Rep*, vol. 2, no. 4, pp. 345–396, Oct. 2005, doi: 10.1007/s10297-005-0054-0.

[3] L. C. Andrews and R. L. Phillips, "Free-space optical communication link and atmospheric effects: single aperture an d arrays," in *Free-Space Laser Communication Technologies XVI*, vol. 5338, pp. 265–275, Jun. 2004, doi: 10.1117/1 2.556737.

[4] A. A. Farid and S. Hranilovic, "Outage Capacity Optimization for Free-Space Optical Links With Pointing Errors," *Journal of Lightwave Technology*, vol. 25, no. 7, pp. 1702–1710, 2007, doi: 10.1109/JLT.2007.899174.

[5] H. G. Sandalidis, T. A. Tsiftsis, G. K. Karagiannidis, and M. Uysal, "BER Performance of FSO Links over Strong Atmospheric Turbulence Channels with Pointing Errors," *IEEE Communications Letters*, vol. 12, no. 1, pp. 44–46, 2008, doi: 10.1109/LCOMM.2008.071408.

[6] R. Ramaswami, K. Sivarajan, and G. Sasaki, *Optical Networks: A Practical Perspective, 3rd Edition*, 3rd edition. Amsterdam ; Boston: Morgan Kaufmann, 2009.

[7] L. F. B. Ribeiro, J. R. F. da Rocha, and O. L. Pinto, "Performance evaluation of EDFA preamplified receivers taking into account intersymbol interference," *Journal of Lightwave Technology*, vol. 13, no. 2, pp. 225–232, 1995, doi: 10.1109/50.365210.

[8] R. S. Fyath and J. J. O'reilly, 'Comprehensive moment generating function characterisation of optically preamplified receivers', *IEE Proceedings J (Optoelectronics)*, vol. 137, no. 6, pp. 391-396, Dec. 1990.

[9] S. D. Personick, "Applications for quantum amplifiers in simple digital optical communication systems," *The Bell System Technical Journal*, vol. 52, no. 1, pp. 117–133, 1973, doi: 10.1002/j.1538-7305.1973.tb03187.x.

[10] D. Marcuse, "Derivation of analytical expressions for the bit-error probability in lightwave systems with optical amplifiers," *Journal of Lightwave Technology*, vol. 8, no. 12, pp. 1816–1823, 1990, doi: 10.1109/50.62876.

  ISSN 2179-1074

[11] Y. Yamamoto, "Noise and error rate performance of semiconductor laser amplifiers in PCM-IM optical transmission systems," *IEEE Journal of Quantum Electronics*, vol. 16, no. 10, pp. 1073–1081, 1980, doi: 10.1109/JQE.1980.1070356.

[12] A. O. Aladeloba, A. J. Phillips, and M. Woolfson, "Improved bit error rate evaluation for optically pre-amplified free-space optical communication systems in turbulent atmosphere," *Optoelectronics, IET*, vol. 6, pp. 26–33, Feb. 2012, doi: 10.1049/iet-opt.2010.0100.

[13] A. O. Aladeloba, A. J. Phillips, and M. S. Woolfson, "DPPM FSO communication systems impaired by turbulence, pointing error and ASE noise," in *2012 14th International Conference on Transparent Optical Networks (ICTON)*, Jul. 2012, pp. 1–4. doi: 10.1109/ICTON.2012.6253854.

[14] J. O'Reilly and J. da Rocha, "Improved error probability evaluation methods for direct detection optical communication systems," *IEEE Transactions on Information Theory*, vol. 33, no. 6, pp. 839–848, 1987, doi: 10.1109/TIT.1987.1057374.

[15] M. R. Hayal, B. B. Yousif, and M. A. Azim, "Performance Enhancement of DWDM-FSO Optical Fiber Communication Systems Based on Hybrid Modulation Techniques under Atmospheric Turbulence Channel," *Photonics*, vol. 8, no. 11, 2021, doi: 10.3390/photonics8110464.

[16] E. E. Elsayed and B. B. Yousif, "Performance enhancement of M-ary pulse-position modulation for a wavelength division multiplexing free-space optical systems impaired by interchannel crosstalk, pointing error, and ASE noise," *Optics Communications*, vol. 475, p. 126219, 2020, doi: https://doi.org/10.1016/j.optcom.2020.126219.

[17] Z. Ghassemlooy, W. Popoola, and S. Rajbhandari, *Optical Wireless Communications: System and Channel Modelling with MATLAB®*, 2nd ed. Boca Raton: CRC Press, 2019. doi: 10.1201/9781315151724.

[18] M. I. Petković and G. T. Đorđević, "Effects of pointing errors on average capacity of FSO links over gamma-gamma turbulence channel," in *2013 11th International Conference on Telecommunications in Modern Satellite, Cable and Broadcasting Services (TELSIKS)*, Oct. 2013, vol. 2, pp. 481–484. doi: 10.1109/TELSKS.2013.6704423.

[19] J. Park, L. Eunju, C.-B. Chae, and G. Yoon, "Impact of Pointing Errors on the Performance of Coherent Free-Space Optical Systems," *IEEE Photonics Technology Letters*, vol. 28, pp. 1–1, Jan. 2016, doi: 10.1109/LPT.2015.2489383.

[20] O. J. Bandele, P. Desai, M. S. Woolfson, and A. J. Phillips, "Saturation in cascaded optical amplifier free-space optical communication systems," *IET Optoelectronics*, vol. 10, no. 3, pp. 71–79, Jun. 2016, doi: 10.1049/iet opt.2015.0083.

[21] M. Razavi and J. H. Shapiro, "Wireless optical communications via diversity reception and optical preamplification," *IEEE Transactions on Wireless Communications*, vol. 4, no. 3, pp. 975–983, May 2005, doi:10.1109/TWC.2005.847102.

[22] A. Hirano, Y. Miyamoto, and S. Kuwahara, "Performances of CSRZ-DPSK and RZ-DPSK in 43-Gbit/s/ch DWDM G.652 single-mode-fiber transmission," in *OFC 2003 Optical Fiber Communications Conference, 2003.*, Mar. 2003, vol.2, pp. 454–456 doi: 10.1109/OFC.2003.315949.

  ISSN 2179-1074